

Thermometry for Laughlin States of Ultracold Atoms

P.T. Raum and V.W. Scarola

Department of Physics, Virginia Tech, Blacksburg, Virginia 24061 USA

(Dated: May 16, 2022)

Cooling atomic gases into strongly correlated quantum phases requires estimates of the entropy to perform thermometry and establish viability. We construct an ansatz partition function for models of Laughlin states of atomic gases by combining high temperature series expansions with exact diagonalization. Using the ansatz we find that entropies required to observe Laughlin correlations with bosonic gases are near current cooling capabilities. Our method can be extended to model cooling into other gapped topological states.

PACS numbers: 03.75.Hh,05.30.Jp,67.85.-d

Observation of the superfluid-to-Mott transition [1, 2] triggered interest in observing other strongly correlated states with ultracold atoms [3, 4]. For example, a proposal [5] to probe models of high temperature superconductors with optical lattices led to efforts to emulate the controversial low temperature phase diagram of the Fermi-Hubbard model [6, 7]. But cooling [8] proved to be a major obstacle. Most atomic gas experiments are closed, to a good approximation. As a result the system entropy determines the temperature. Temperature is difficult to characterize in a strongly correlated regime because entropy-temperature relationships derive from non-trivial many-body effects. Relatively recent theoretical work [9–12] showed that the critical entropy to realize the best case scenario for emulation, the Néel state, lies below current cooling capabilities [8]. In the case of the Fermi-Hubbard model, the entropy-temperature relationship proved to be unfavorable for realizing low temperatures at available entropies. From this example we see the importance of estimates of thermodynamic functions of proposed states in defining thermometry and establishing viability.

A separate class of proposals seek to realize fractional quantum Hall (FQH) states of atoms, particularly Laughlin states [13], which, at low energies, have intriguing excitations with anyon statistics that define them as topological [14]. These proposals rely on schemes to implement strong artificial magnetic fields (See Refs. [3, 4, 15–20] for reviews). Experiments using rotation [21–26] or phase imprinting [27–36] have shown considerable progress. But the thermodynamic relations needed for thermometry of large FQH systems are currently unknown.

The Laughlin state energy gap establishes a Schottky-type peak in the heat capacity. In a naive non-interacting model of gapped excitations an entropy per particle below $\approx 0.29k_B$ is needed to lower the temperature below the heat capacity peak for bosons, assuming the known energy gap for bosonic Laughlin states [37]. This low entropy is currently well out of reach of evaporative cooling methods [8]. A more accurate estimate of the entropy, incorporating the non-trivial excited state spectra

of Laughlin states, is needed to establish viability of low temperature FQH states with atomic gases.

Analyses of non-perturbative FQH models rely on a combination of numerics and ansatz theories. Exact diagonalization has been used to compute the heat capacity over the entire temperature range but only for small systems [38, 39]. Other work has examined the thermodynamics of infinite system sizes using series expansions [40–42] but these studies are restricted to temperatures much larger than the gap. Ansatz theories [43], building on the success of the composite fermion (CF) wavefunctions [44, 45] at describing the low energy excitations [46], offer estimates for thermodynamic functions only at low temperatures. A theory for the entropy-temperature relationship over the complete temperature range in large systems is necessary for guiding atomic gas experiments as they cool into FQH states.

We construct a theory of Laughlin state thermodynamics using an ansatz partition function. We design the ansatz to be exact at high temperatures, to capture the low temperature asymptotics, and to be straightforward to use, thus allowing characterization of the entire temperature range. We establish a numerical validation procedure (which combines a high temperature series expansion with the stochastic trace method [47]) to compare our ansatz against exact results where possible. Using our ansatz we incorporate the excited state structure of FQH states [44–46] to find that, in contrast to the naive estimate for a gapped system, entropies currently accessible with bosonic gases [8] are nearly low enough to probe the low temperature properties of Laughlin states. Remarkably, the energy distribution of the excited states effectively lowers the temperature of the Schottky-type peak at fixed entropy in comparison to the naive estimate. Our method can be used to construct thermodynamic functions of other FQH states and gapped topological states in general.

Model: We consider a Hamiltonian of N particles of mass M in two-dimensions subjected to an artificial magnetic

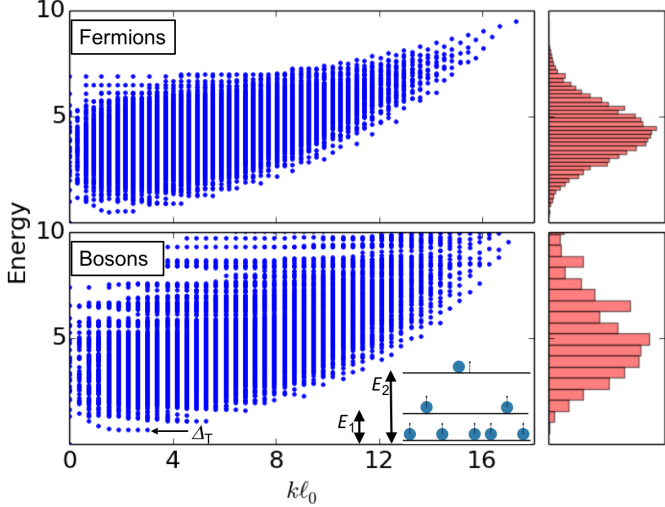


Figure 1. Energy of $N = 8$ fermions (bosons) at $\nu = 1/3$ ($\nu = 1/2$) as a function of total wavevector for $n = 1$ ($n = 0$) in Eq. (1) in the lowest Landau level. The ground state is the $k = 0$ Laughlin state set to zero energy. Δ_T is the transport gap. The schematic depicts example excitations. The bosonic Laughlin state can be thought of as one filled level of CFs (bosons attached to one flux quantum). Low energy excitations are CF particle-hole pairs modeled as excitations with energy $E_1 \sim \Delta_T$. We consider additional excitations at another characteristic energy, E_2 , where bosons are not necessarily bound to flux quanta. The histograms show nearly Gaussian state counting.

field oriented perpendicular to the $x - y$ plane:

$$H = \sum_{i=1}^N \left[\frac{|\mathbf{p}_i - q^* \mathbf{A}_i/c|^2}{2M} + \frac{M(\omega^2 - \Omega^2)}{2} r_i^2 \right] + b_n \sum_{i < j}^N \nabla^{2n} \delta(\mathbf{r}_i - \mathbf{r}_j), \quad (1)$$

where \mathbf{p}_i is the planar momentum, $\mathbf{A}_i = (\mathbf{B}^* \times \mathbf{r}_i)/2$ is the vector potential in the symmetric gauge, $\Omega \equiv q^* B^*/2M$, $\mathbf{r}_i = (x_i, y_i)$, and B^* (q^*) is the artificial magnetic field (charge). The effective magnetic length is $l_0 = (\hbar c/q^* B^*)^{1/2}$. In this gauge the concentric ring-like basis states define the disk geometry. Here we have assumed a strong trap along the z -direction and an external parabolic confinement in the $x - y$ plane with a trapping frequency ω . We leave a discussion of edges to the end and focus on bulk states. We set $\omega = \Omega$ and work in units of $l_0 = k_B = 1$. An s -wave (p -wave) interaction for $n = 0$ ($n = 1$) generates repulsion. Setting $b_n = 1$ defines our energy unit.

H approximates several physical systems proposed for realizing FQH states with ultracold atoms. We consider an atomic gas with a known entropy that is adiabatically loaded into a setup designed to generate $q^* B^*$. For example, a rotating gas generates $q^* B^*$ from the Coriolis force

[15, 48]. Artificial gauge fields in lattices offer another example. H becomes accurate even in lattices when the flux through each unit cell is small (see, e.g., Ref [49]).

In all proposals the magnetic field must be large enough to restrict states to the lowest Landau level. In this approximation the Laughlin state is the exact ground state of Eq. (1) for bosons (fermions) with $n = 0$ ($n = 1$) at $\nu = 1/2$ ($1/3$), where ν is the filling factor, the number of particles per flux quanta [50, 51]. In the following, when referring to bosons and fermions, we imply results at $\nu = 1/2$ and $\nu = 1/3$ with $n = 0$ and $n = 1$, respectively.

The Laughlin states form a subset of a larger class of states, the CF states, that accurately capture the low energy physics. We think of a CF as a weakly interacting quasiparticle defined by attaching flux quanta to the original particles. The Laughlin ground state becomes a filled effective level of CFs. Low energy excitations are then particle-hole pairs of CFs (See the schematic inset to Fig. 1).

To study thermodynamics over the entire temperature range we use Eq. (1) to compute the energy versus total wavevector in the spherical geometry, the geometry we use throughout. The spherical geometry maps to the disk geometry in the $N \rightarrow \infty$ limit [50, 52, 53] and allows us to focus on bulk states. Fig. 1 shows a gap to a set of low energy modes, CF particle-hole pairs. But the high energy states form a continuum which contribute significantly to the thermodynamics.

We take a statistical approach to incorporating the high energy continuum into the thermodynamics. The histograms in Fig. 1 plot the distribution of energies. The observation that the continuum forms a nearly Gaussian distribution will form the basis for our ansatz.

The peaks in the high energy tail of the boson distribution in Fig. 1 arise from large vortex states. To see this note that the highest energy states of the repulsive model studied here can be thought of as the low energy states in an attractive model ($b_0 < 0$). Ref. [54] shows that attractive bosons form large vortices which therefore lead to the histogram peaks in Fig. 1.

Figure 1 shows only the neutral excitations. In solids nearby particle reservoirs lead to addition or subtraction of additional particles (charged excitations) but in trapped atomic gases particle number is essentially fixed. We therefore focus our analysis to neutral excitations.

Figure 1 also excludes center of mass excitations and plots energies of excitations built from relative coordinates. H separates into relative and center of mass coordinates. The total partition function in the canonical ensemble becomes: $Z_{\text{TOT}} = Z_{\text{CM}} \times Z$, where Z_{CM} (Z) is the partition function for the center of mass (relative) coordinates. In the following we assume a fixed center of mass and focus on approximating Z for neutral excitations in the bulk.

Method: To approximate the thermodynamics of Laugh-

	fermions	bosons
Δ_T	0.428(6)	0.627(3)
κ_0/N	1.899(1)	1.899(1)
κ_1/N	0.66645(3)	1.006(5)
κ_2/N	0.2975(2)	2.28(2)
κ_3/N	0.0854(2)	25.5
κ_4/N	0.0017(3)	$7.1(2) \times 10^2$
κ_5/N	0.150(2)	$3.5(2) \times 10^2$

Table I. The first row shows the transport gap and the remaining rows the cumulants for fermions (bosons) at $\nu = 1/3$ ($\nu = 1/2$) for $n = 1$ ($n = 0$) in Eq. (1). All results are obtained by finite size scaling of exact numerical results to the thermodynamic limit [55].

in states we construct an ansatz partition function which captures the exact thermodynamics at high temperatures and has the correct temperature dependence at low temperatures. Through fitting to our numerically derived data we arrive at an approximate partition function applicable over the entire temperature range.

Motivated by the Gaussian-like energy distribution we consider the following ansatz partition function:

$$Z_A \equiv \left(1 + g_1 e^{-E_1/T} + g_2 e^{-E_2/T}\right)^N, \quad (2)$$

where g_l and E_l are fitting parameters. The second term in the partition function defines the low T dependence of a gapped spectrum (for $E_1 < E_2$). The lowest energy excitation shown in Fig. 1 is k -dependent but we find that including k -dependence in E_l does not alter our results. We therefore ignore k -dependence and expect $E_1 \sim \Delta_T$, where Δ_T is the transport gap. Furthermore, $g_1 \sim 1$ approximates the degeneracy of the first excitation.

We capture additional states in the high energy spectrum with the third term. The inset to Fig. 1 schematically depicts another energy level, E_2 , where flux quanta are not necessarily bound to particles. At very high energies we expect states that do not involve flux attachment to play a role.

To fix parameters in the ansatz we consider an exact high temperature expansion related to the free energy:

$$\log Z = \sum_{l=0}^{\infty} \kappa_l (-T)^{-l} / l!, \quad (3)$$

defined in terms of the cumulants, κ_l . The lowest cumulants have simple interpretations, e.g., κ_0 is the log of the size of the Hilbert space. Stirling's formula leads to $\kappa_0/N = 3\log(3) - 2\log(2)$ for $N \rightarrow \infty$. Also, $\kappa_1/N = \text{Tr}(H)/N$ becomes 2ν [42]. Table I shows the cumulants we find in the $N \rightarrow \infty$ limit using finite size scaling of numerically exact results obtained from the stochastic trace method [55].

We use the cumulants from the high temperature ex-

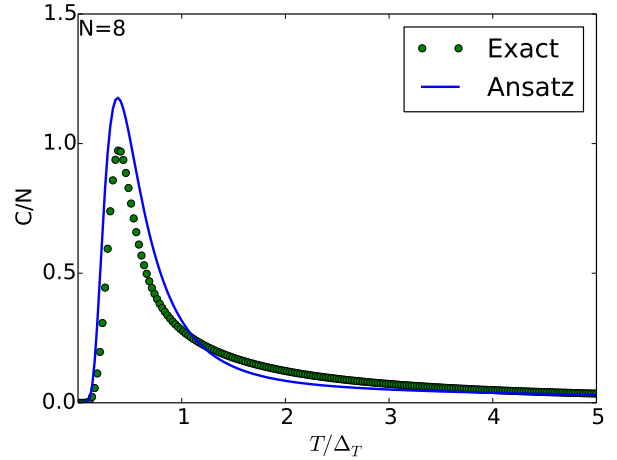


Figure 2. Heat capacity versus temperature for $N = 8$ bosons. The symbols are obtained from diagonalization of Eq. (1) and the solid line follows from the ansatz partition function, Eq. (2). The ansatz parameters were obtained by fitting the lowest four cumulants for $N = 8$. The agreement at high T follows by construction but the low T agreement demonstrates the accuracy of the ansatz.

pansion to fix the parameters in Z_A . We apply our method to bosons and reserve an analysis of fermions for future work because $n = 1$ in Eq. (1) requires strong p -wave scattering which is experimentally challenging with alkali atoms. We use a Groebner basis fit to the high temperature limit. We find: $g_1 = 5.61(4)$, $E_1 = 0.970(6)$, $g_2 = 0.099(4)$, and $E_2 = 13.1(2)$. The error in our cumulant fits were propagated through our fitting procedure. With these parameters we reproduce the exact high temperature partition function [up to $\mathcal{O}(T^{-4})$].

We test the accuracy of the fits by including more fitting parameters. We have included additional terms to fit up to $\mathcal{O}(T^{-6})$ with more fitting parameters, e.g., $g_3 e^{-E_3/T}$, in Z_A and have found that our results for fitting parameters change very little, e.g., the entropy changes by less than 1% percent. We therefore keep our 4 parameter ansatz.

Thermodynamic Functions: To test the validity of the ansatz partition function we compare with exact diagonalization results for thermodynamic functions. We compare directly on small system sizes and for the thermodynamic limit where possible.

Figure 2 plots the heat capacity, $C = T \partial S / \partial T$, where $S = \partial(T \log Z) / \partial T$ is the entropy. We compare C obtained from exact diagonalization and from the ansatz. In this example comparison we see that both the high and low T limits agree. The former is by construction but the latter is non-trivial because we fit just the high T limit. The low T limit of the gapped system contains information about the degeneracy of the first excited level, g_1 , since for a system with a gap Δ_T and degeneracy g we have: $C/N = [g(\Delta_T/T)^2 + \mathcal{O}(T^3)]e^{-\Delta_T/T}$. We also find that increasing N improves agreement between diagonal-

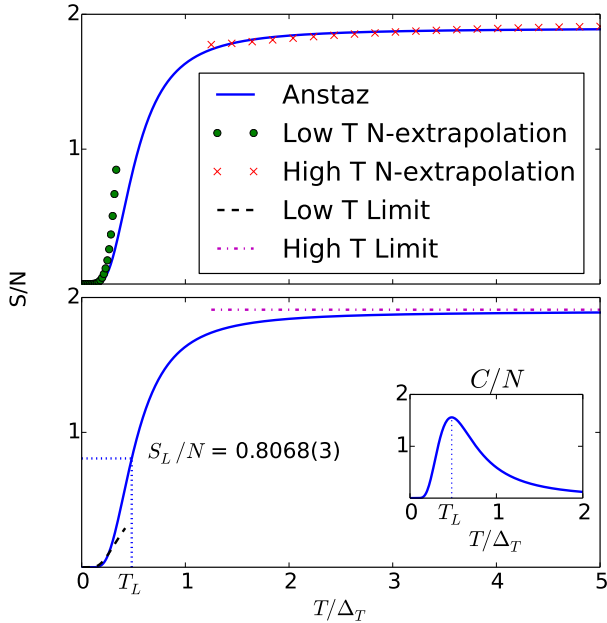


Figure 3. The main panels plot the entropy per particle versus temperature for bosons. The solid lines are obtained from the ansatz, Eq. (2), with parameters derived from the cumulants in Table I. The symbols in the top panel are obtained from finite N extrapolation of the entropy at fixed T [55]. The agreement between the symbols and the lines shows that the ansatz accurately captures the low and high T limits. The dashed line in the bottom panel plots the entropy per particle obtained from a partition function $[1 + \exp(-\Delta_T/T)]^N$. The dot-dashed line plots the high T limit from the first term of the cumulant expansion ($S = \kappa_0$). The inset plots the heat capacity from the ansatz in the thermodynamic limit. The vertical dotted line denotes the temperature, T_L , below which primarily CF particle-hole pairs are excited. The horizontal dotted line in the main panel plots the corresponding entropy, S_L , determined from the ansatz.

ization and the ansatz near the peak.

We also test Z_A in the thermodynamic limit. We study the entropy because of its importance in atomic gas thermometry. We use exact diagonalization at finite N . We fix T and use finite size scaling to obtain the entropy. The supplementary material [55] discusses finite-size scaling functions of the entropy at very low T and very high T . For $T \sim \Delta_T$ we cannot predict an N scaling function.

The top panel of Fig. 3 plots a comparison between the entropy obtained from Z_A and the results for finite-size scaling of the entropy. Here we see that the ansatz agrees well with the extrapolations at low and high T . The bottom panel of Fig. 3 plots a comparison between the entropy obtained from Z_A and two limits: the low T limit obtained from assuming a two-level system with a gap Δ_T and the high T limit from the first term of the cumulant expansion ($S = \kappa_0$). The deviation between the dashed and solid lines shows the importance of incorporating the continuum states even for $T \sim \Delta_T/5$. In both panels we see that the ansatz extrapolates between

both low and high T limits thus allowing predictions for thermodynamic functions even for $T \sim \Delta_T$.

Laughlin Entropy: We use the validated ansatz to predict the thermodynamic entropy at which Laughlin correlations set in. Although there is no critical temperature in the FQH regime we consider a characteristic temperature, T_L , defined as the temperature at which the heat capacity peaks due to the energy gap. At the peak we find an excitation fraction of $\approx 19\%$ from our boson ansatz.

The inset of Fig. 3 plots the ansatz heat capacity versus temperature to reveal the location of the peak and therefore T_L . The bottom panel of Fig. 3 shows the entropy that corresponds to the peak in the heat capacity, S_L . We find $S_L/N \approx 0.8068(3)$, where the error propagates from uncertainty in the ansatz fitting parameters. This entropy is much larger than the naive estimate mentioned in the introduction therefore showing the cooling effect of the continuum of excited states. The entropy found here establishes a bound on the entropy needed to reliably observe the low- T /CF physics of the FQH regime with bosons.

Experimental Implications: Our estimate for the entropy needed to observe FQH states with bosons is near current cooling capabilities. Evaporative cooling can reach entropies as low as $S/N \approx 0.35$ and possibly lower [8] which, according to the ansatz, corresponds to $T \approx 0.5T_L$. We have therefore found that the entropy per particle required to lower the system temperature below T_L is within reach of current cooling capabilities. The ansatz shows that $T \approx 0.5T_L$ still allows an excitation fraction of $\approx 1\%$. Cooling to $T \lesssim 0.1T_L$ would be optimal for probes of ground state properties and consistent with temperatures in solids.

Our estimates here only apply to neutral excitations within the bulk in the thermodynamic limit whereas including edge effects or additional quasiparticles can lower T at fixed S (adiabatic cooling) in finite sized systems. Introducing edges in a finite sized experiment should make the entropy budget more favorable for observing FQH physics. For $\Omega \neq \omega$ edge states interplay with parabolic trapping in finite sized systems. The (nearly) gapless edge states accommodate more entropy than the bulk [an $\mathcal{O}(\sqrt{N})$ effect]. Introducing edges should therefore adiabatically lower temperature. Our estimate for S_L in the thermodynamic limit is then a *lower bound* on the entropy needed to reach low temperature FQH states in a finite size experiment.

Moving the filling away from $1/(1+p)$ introduces quasiparticles to allow additional cooling. The topological nature of Laughlin states implies that the total entropy includes a factor due to quasiparticle degeneracy, yielding: $S_D + S$, where $S_D = N_q \log(d)$, $d = \sqrt{p+1}$ is the quantum dimension, and N_q is the number of additional quasiparticles causing deviation from filling $1/(1+p)$ [14]. The T -independent S_D term allows adiabatic cooling via quasiparticles [56].

Summary: We have constructed and validated an ansatz partition function for Laughlin states with atomic gases. Our method leads to an ansatz that is exact at temperatures much higher than the gap and contains the correct T dependence at low temperatures thus allowing thermometry through the entire temperature range. Using our ansatz we find that the continuum of excited states alters the entropy-temperature relationship (in comparison to that of a naive gapped spectrum) to reveal that currently attainable entropies are nearly low enough to observe low temperature FQH states with bosons. Our results also have important implications for observing other closely related topological states, e.g., chiral spin liquids and fractional Chern insulators, because of their direct connection to the bosonic Laughlin state [57, 58].

We acknowledge helpful comments from M. Peterson and support from the AFOSR (FA9550-11-1-0313) and ARO (W911NF-16-1-0182).

[1] D. Jaksch, C. Bruder, J. I. Cirac, C. W. Gardiner, and P. Zoller, *Phys. Rev. Lett.* **81**, 3108 (1998).

[2] M. Greiner, O. Mandel, T. Esslinger, T. W. Hansch, and I. Bloch, *Nature* **415**, 39 (2002).

[3] I. Bloch, J. Dalibard, and W. Zwerger, *Rev. Mod. Phys.* **80**, 885 (2008).

[4] M. Lewenstein, A. Sanpera, and V. Ahufinger, *Ultracold Atoms in Optical Lattices: Simulating quantum many-body systems* (OUP Oxford, 2012).

[5] W. Hofstetter, J. I. Cirac, P. Zoller, E. Demler, and M. D. Lukin, *Phys. Rev. Lett.* **89**, 220407 (2002).

[6] A. Cho, *Science* **320**, 312 (2008).

[7] T. Esslinger, *Ann. Rev. of Condens. Matt. Phys.* **1**, 129 (2010).

[8] D. C. McKay and B. DeMarco, *Rep. Prog. Phys.* **74**, 054401 (2011).

[9] A. Koetsier, R. A. Duine, I. Bloch, and H. T. C. Stoof, *Phys. Rev. A* **77**, 023623 (2008).

[10] S. Fuchs, E. Gull, L. Pollet, E. Burovski, E. Kozik, T. Pruschke, and M. Troyer, *Phys. Rev. Lett.* **106**, 030401 (2011).

[11] T. Paiva, Y. L. Loh, M. Randeria, R. T. Scalettar, and N. Trivedi, *Phys. Rev. Lett.* **107**, 086401 (2011).

[12] E. Kozik, E. Burovski, V. W. Scarola, and M. Troyer, *Phys. Rev. B* **87**, 205102 (2013).

[13] R. Laughlin, *Phys. Rev. Lett.* **50**, 1395 (1983).

[14] C. Nayak, S. H. Simon, A. Stern, M. Freedman, and S. Das Sarma, *Rev. Mod. Phys.* **80**, 1083 (2008).

[15] N. R. Cooper, *Adv. Phys.* **57**, 539 (2008).

[16] S. Viefers, *J. Phys.: Condens. Matter* **20**, 123202 (2008).

[17] C. Salomon, G. V. Shlyapnikov, and L. F. Cugliandolo, *Many-Body Physics with Ultracold Gases: Lecture Notes of the Les Houches Summer School: Volume 94, July 2010* (Oxford University Press, 2013).

[18] J. Dalibard, F. Gerbier, G. Juzeliūnas, and P. Öhberg, *Rev. Mod. Phys.* **83**, 1523 (2011).

[19] N. Goldman, G. Juzeliūnas, P. Öhberg, and I. B. Spielman, *Rep. Prog. Phys.* **77**, 126401 (2014).

[20] N. Goldman, J. C. Budich, and P. Zoller, *Nat. Phys.* **12**, 639 (2016).

[21] K. W. Madison, F. Chevy, W. Wohlleben, and J. Dalibard, *Phys. Rev. Lett.* **84**, 806 (2000).

[22] J. R. Abo-Shaeer, C. Raman, J. M. Vogels, and W. Ketterle, *Science* **292**, 476 (2001).

[23] V. Bretin, S. Stock, Y. Seurin, and J. Dalibard, *Phys. Rev. Lett.* **92**, 050403 (2004).

[24] V. Schweikhard, I. Coddington, P. Engels, V. Mogen-dorff, and E. Cornell, *Phys. Rev. Lett.* **92**, 040404 (2004).

[25] S. Tung, V. Schweikhard, and E. A. Cornell, *Phys. Rev. Lett.* **97**, 240402 (2006).

[26] N. Gemelke, E. Sarajlic, and S. Chu, (2010), [arxiv:1007.2677](https://arxiv.org/abs/1007.2677).

[27] Y. J. Lin, R. L. Compton, A. R. Perry, W. D. Phillips, J. V. Porto, and I. B. Spielman, *Phys. Rev. Lett.* **102**, 130401 (2009).

[28] Y. J. Lin, R. L. Compton, K. Jimenez-Garcia, J. V. Porto, and I. B. Spielman, *Nature* **462**, 628 (2009).

[29] M. Aidelsburger, M. Atala, S. Nascimbène, S. Trotzky, Y. Chen, and I. Bloch, *Phys. Rev. Lett.* **107**, 255301 (2011).

[30] L. J. LeBlanc, K. Jimenez-Garcia, R. A. Williams, M. C. Beeler, A. R. Perry, W. D. Phillips, and I. B. Spielman, *Proc. of the Nat. Acad. of Sci.* **109**, 10811 (2012).

[31] J. Struck, C. Ölschläger, M. Weinberg, P. Hauke, J. Simonet, A. Eckardt, M. Lewenstein, K. Sengstock, and P. Windpassinger, *Phys. Rev. Lett.* **108**, 225304 (2012).

[32] M. Aidelsburger, M. Atala, M. Lohse, J. T. Barreiro, B. Paredes, and I. Bloch, *Phys. Rev. Lett.* **111**, 185301 (2013).

[33] H. Miyake, G. A. Siviloglou, C. J. Kennedy, W. C. Burton, and W. Ketterle, *Phys. Rev. Lett.* **111**, 185302 (2013).

[34] M. Atala, M. Aidelsburger, M. Lohse, J. T. Barreiro, B. Paredes, and I. Bloch, *Nat. Phys.* **10**, 588 (2014).

[35] B. K. Stuhl, H. Lu, L. M. Aycock, D. Genkina, and I. B. Spielman, *Science* **349**, 1514 (2015).

[36] C. J. Kennedy, W. C. Burton, W. C. Chung, and W. Ketterle, *Nat. Phys.* **11**, 859 (2015).

[37] T. Nakajima and M. Ueda, *Phys. Rev. Lett.* **91**, 140401 (2003).

[38] D. Yoshioka, *J. Phys. Soc. Jpn.* **56**, 1301 (1987).

[39] T. Chakraborty and P. Pietiläinen, *Phys. Rev. B* **55**, R1954 (1997).

[40] L. Zheng and A. MacDonald, *Surf. Sci.* **305**, 101 (1994).

[41] K. Tevosyan and A. H. MacDonald, *Phys. Rev. B* **56**, 7517 (1997).

[42] S. Sawatdiaree and W. Apel, *Physica E* **6**, 75 (2000).

[43] G. Murthy and R. Shankar, *Rev. Mod. Phys.* **75**, 1101 (2003).

[44] J. Jain, *Phys. Rev. Lett.* **63**, 199 (1989).

[45] J. Jain, *Composite fermions* (Cambridge University Press, 2007).

[46] J. Jain, K. Park, M. Peterson, and V. Scarola, *Solid State Commun.* **135**, 602 (2005).

[47] A. Weisse, G. Wellein, A. Alvermann, and H. Fehske, *Rev. Mod. Phys.* **78**, 275 (2006).

[48] N. Wilkin and J. Gunn, *Phys. Rev. Lett.* **84**, 6 (2000).

[49] A. Sorensen, E. Demler, and M. Lukin, *Phys. Rev. Lett.* **94**, 086803 (2005).

[50] F. Haldane, *Phys. Rev. Lett.* **51**, 605 (1983).

[51] S. Trugman and S. Kivelson, *Phys. Rev. B* **31**, 5280 (1985).

- [52] G. Fano, F. Ortolani, and E. Colombo, *Phys. Rev. B* **34**, 2670 (1986).
- [53] A. Wójcik and J. J. Quinn, *Physica E* **3**, 181 (1998).
- [54] N. K. Wilkin, J. M. F. Gunn, and R. A. Smith, *Phys. Rev. Lett.* **80**, 2265 (1998).
- [55] See the Supplemental Material.
- [56] G. Gervais and K. Yang, *Phys. Rev. Lett.* **105**, 086801 (2010).
- [57] V. Kalmeyer and R. Laughlin, *Phys. Rev. Lett.* **59**, 2095 (1987).
- [58] N. Y. Yao, A. V. Gorshkov, C. R. Laumann, A. M. Läuchli, J. Ye, and M. D. Lukin, *Phys. Rev. Lett.* **110**, 185302 (2013).

SUPPLEMENTARY MATERIAL FOR “THERMOMETRY FOR LAUGHLIN STATES OF ULTRACOLD ATOMS”

Stochastic Trace Method

This section outlines a method to numerically compute the cumulants. We first note that the cumulants are related to the moments of the Hamiltonian, $\text{Tr}(H^l)$, via:

$$\kappa_l = \text{Tr}(H^l) - \sum_{l'=1}^{l-1} \binom{l-1}{l'-1} \kappa_{l'} \text{Tr}(H^{l-l'}), \quad (4)$$

for $l > 0$. This expression allows us to estimate the cumulants with moments. Consider R normalized random vectors $|r\rangle$ in the Hilbert space. The moments can then be estimated using:

$$\text{Tr}(H^l) \approx R^{-1} \sum_{r=0}^{R-1} \langle r | H^l | r \rangle. \quad (5)$$

We obtain convergence in the sum by choosing $R = 100$ random vectors. The error in this method scales like $\mathcal{O}[(RD)^{-1/2}]$ where, D is the size of the Hilbert space. For $N = 12$ we achieve errors of less than $\sim 10^{-6}$ and have compared with exact diagonalization where possible. We therefore find that the stochastic trace method is numerically exact.

Finite-Size Scaling

This section discusses finite size scaling forms used for the cumulants and the entropy. To extrapolate the cumulants to the $N \rightarrow \infty$ limit we use different scaling functions. The functions are used to fit numerical data.

We use three different scaling functions for the cumulants. For κ_0 , which is the log of the dimension size, we use Stirling's formula to extract the following large N scaling:

$$\frac{\kappa_0}{N} \sim a + \frac{b}{N} + \frac{c}{2N} \log\left(\frac{1}{N}\right), \quad (6)$$

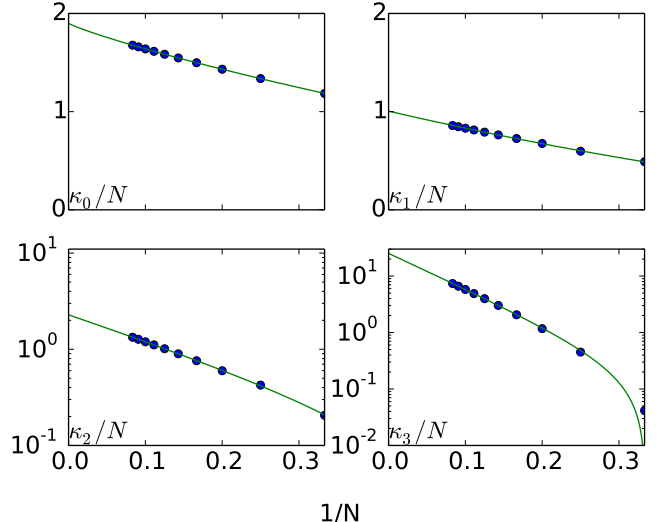


Figure 4. The symbols are boson cumulants per particle obtained from the numerically exact stochastic trace method. The lines show finite size scaling functions Eqs. (6), (7), and (8). κ_0 is the log of the Hilbert space size and exhibits a log-linear N scaling. κ_1 fits to a polynomial while $\kappa_{l>1}$ fit to an exponential. The thermodynamic limit ($N \rightarrow \infty$) of these values is given in Table I in the main text.

where a, b and c are fitting parameters obtained from fitting our numerical data. For κ_1 we use a standard finite size scaling function used for energy extrapolations in FQH studies:

$$\frac{\kappa_1}{N} \sim a + \frac{b}{N} + \frac{c}{N^2}, \quad (7)$$

but for higher order cumulants we find that an exponential scaling yields the least error in fitting:

$$\frac{\kappa_{l>2}}{N} \sim a + b \exp[c/N]. \quad (8)$$

Figure 4 shows example numerical extrapolations for boson cumulants using the stochastic trace method. Fits for bosons for κ_0/N and κ_1/N yield $1.899(1)$ and $1.006(5)$, respectively, close to our expected values, ≈ 1.90954 and 1.0 , thus confirming that our fitting protocol extrapolates well to $N \rightarrow \infty$. The $N \rightarrow \infty$ limit we find for cumulants is given in Table I in the main text.

We also perform finite size scaling of thermodynamic functions directly. The dashed and dot-dashed lines in the bottom panel of Fig. 3 in the main text shows the entropy per particle extrapolated to $N \rightarrow \infty$ for several T . To obtain the results presented in Fig. 3 in the main text we performed finite size scaling of the entropy. The finite size scaling of the entropy per particle is well defined at very low T and very high T . For $T \ll \Delta_T$ we

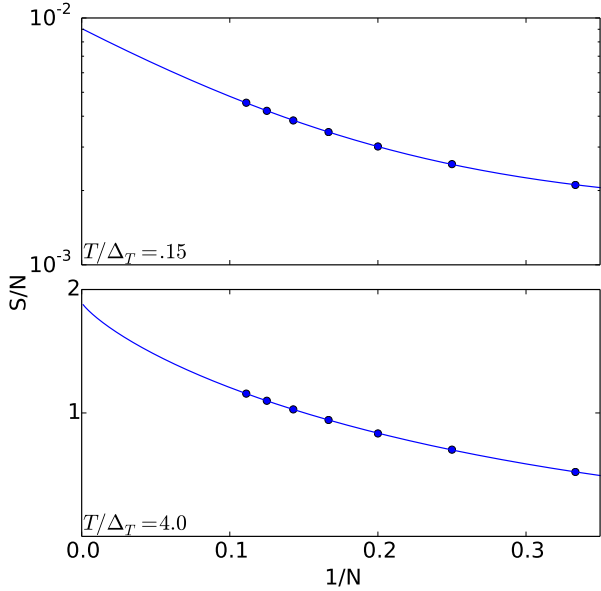


Figure 5. Finite-size extrapolation of the entropy per particle for two different temperatures, $T/\Delta_T = 0.15$ (top panel) and $T/\Delta_T = 4$ (bottom panel). The symbols show results from exact diagonalization for bosons at $\nu = 1/2$ and the solid lines are fitting functions, Eq. (9) (top panel) and Eq. (10) (bottom panel).

find an exponential scaling:

$$\left. \frac{S}{N} \right|_{T \ll \Delta_T} \sim \tilde{a}(T) + \tilde{b}(T) \exp[\tilde{c}(T)/N], \quad (9)$$

where the tilde indicates temperature dependence in the fitting parameters \tilde{a} , \tilde{b} , and \tilde{c} . The high temperature N -scaling of the entropy is different. For $T \gg \Delta_T$ Sterling's formula leads to a log-linear scaling for the entropy:

$$\left. \frac{S}{N} \right|_{T \gg \Delta_T} \sim \tilde{a}(T) + \frac{\tilde{b}(T)}{N} + \frac{\tilde{c}(T)}{2N} \log\left(\frac{1}{N}\right). \quad (10)$$

Here we note that at infinite T the entropy becomes just the log of the Hilbert space size, κ_0 . We have checked that our finite size scaling form for the entropy extrapolates to the log of the Hilbert space size for infinite T .

Fig. 5 shows example N scalings for the entropy for two different temperatures. The top panel uses a log-linear plot to show an extrapolation using the exponential form, Eq. (9), for a characteristic low T . The bottom panel shows an extrapolation using the log-linear form, Eq. (10), for a characteristic high T . In both panels we see that the finite size numerical data fall on the extrapolation lines. Intermediate temperatures ($T \sim \Delta_T$) were not accessible because the fitting functions fail to capture numerical data. We are therefore limited to low and high T results for this method. In these low and high T regimes we then use the extrapolated values of the entropy to compare with the ansatz, all in the $N \rightarrow \infty$ limit. Specifically, the dashed and dot-dashed lines in the bottom panel of Fig. 3 in the main text plot the y -intercept obtained from fits at different temperatures as shown in Fig. 5.